Accelerated Iterative Calculation of Transonic Nacelle Flowfields

D.A. Caughey*
McDonnell Douglas Corporation, St. Louis, Mo.
and
Antony Jameson†
New York University, New York, N.Y.

A method is presented for the calculation of inviscid, supercritical flowfields about axisymmetric inlet cowls. A finite-difference calculation is performed in a simple, rectangular domain obtained from the nacelle geometry by a nearly conformal mapping procedure. Type-dependent finite differences are constructed using a coordinate-independent, "rotated" differencing scheme. Methods of accelerating convergence of the iterative solution are demonstrated including a hybrid fast-Poisson-solver/relaxation scheme and an extrapolated relaxation procedure. Calculated pressure distributions are compared with experimental data for a variety of Mach numbers and mass flow ratios, and show generally good agreement.

Introduction

In recent years, finite-difference methods have been successful in predicting the inviscid, supercritical flowfields about increasingly complex configurations of aerodynamic interest. Murman and Cole[1] originated the idea of type-dependent differencing for transonic flow calculations, applying the technique to the airfoil problem using the transonic small-disturbance equation. The airfoil problem was treated using the full potential equation by Korn and Garabedian[2] and by Jameson,[3] who also included bodies of revolution. Ballhaus and Bailey[4] have treated three-dimensional wings within the framework of small-disturbance theory, and Jameson[5] has treated the same problem using the full potential equation, introducing a "rotated" differencing scheme to allow greater freedom in the choice of coordinate grids.

We are concerned here with the application of these iterative, finite-difference techniques to the calculation of the transonic flowfield about an inlet cowl, or nacelle. This problem has been treated by Colehour,[6] who used the incompressible streamlines to generate a coordinate system. This simplifies the construction of a stable iterative scheme but introduces a singularity that forces the compressible and incompressible stagnation points to coincide. An analysis also has been given by Arlinger.[7] He used a sequence of conformal mappings to generate a rectangular computational domain and a relaxation scheme to solve the system of equations resulting from a finite-difference approximation which an upwind bias which was introduced in the local flow direction at supersonic points.

Our approach is similar in concept to Arlinger's; however, there are two main differences. First, our calculations are performed in a slighly nonorthogonal coordinate system that is obtained from the nacelle geometry much more simply by a slight shearing of a simple, analytically performed conformal mapping. Second, we have demonstrated several methods of accelerating the convergence of the iterative scheme for solving the finite-difference equations. These methods are particularly useful if convergence to very small residuals is desired.

The geometry of the problem under consideration is shown in Fig. 1. The nacelle is treated as a semi-infinite body, extending to downstream infinity as a tube of constant wall thickness. The inside cross-sectional area at infinity is denoted by A_{cf}; the reference area of the nacelle, taken to be that defined by the leading-edge radius, is denoted by A_{hl}, and the capture area is denoted by A_0. The conventionally defined mass flow ratio is given by A_0/A_{hl}. The freestream is assumed to be uniform at infinity outside the nacelle, having a Mach number M_∞, and again uniform in the axial direction at infinity inside the nacelle, with velocity $(1+k)$ that of the freestream.

Analysis

Potential Equation

The analysis here is based upon the potential equation for steady flow, which is accepted as an accurate approximation to the Euler equations of inviscid flow in the absence of strong shock waves. Furthermore, our analysis is based upon differencing this equation in nonconservative form. This approach does not yield the proper jump conditions across shocks appearing in the solution,[8,9] but results obtained from such calculations generally agree well with experimental data, probably because the error thus introduced tends to be cancelled by that resulting from neglect of the shock-wave/boundary-layer interaction,[10] for which no satisfactory solution yet exists. In the present analysis, no account is taken of the displacement effect of the boundary layer. When a

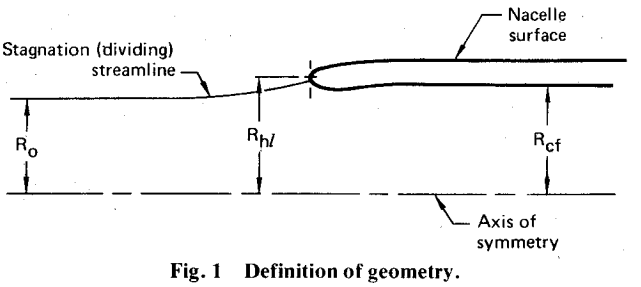

Fig. 1 Definition of geometry.

Presented as Paper 76-100 at the AIAA 14th Aerospace Sciences Meeting, Washington, D.C., January 26-28, 1976; submitted Feb. 3, 1977; revision received July 7, 1977.

Index categories: Transonic Flow; Computational Methods; Aerodynamics.

*Scientist, Flight Sciences Department, McDonnell Douglas Research Laboratories; currently Assistant Professor, Sibley School of Mechanical and Aerospace Engineering, Cornell University, Ithaca, N.Y. Member AIAA.

†Professor of Computer Science, Courant Institute of Mathematical Sciences. Member AIAA.

conservation form of the equation is used, it is generally more important to account for boundary-layer displacement effects, especially in the vicinity of shock waves.

In cylindrical polar coordinates, the equation for the velocity potential ϕ describing axisymmetric, steady flow can be written as

$$(a^2-u^2)\phi_{xx}-2uv\phi_{xr}+(a^2-v^2)\phi_{rr}+a^2v/r=0 \tag{1}$$

where $u=\phi_x$, $v=\phi_r$, and a is the local speed of sound, determined from the energy equation

$$a^2=a_0^2-(\gamma-1)(u^2+v^2)/2 \tag{2}$$

where γ is the ratio of specific heats for the assumed calorically perfect gas, and a_0 is the stagnation speed of sound. On the axis $r=0$, Eq. (1) is singular, and we must use the fact that

$$v=0+r\phi_{rr}+O(r^2)$$

to arrive at the special form

$$(a^2-u^2)\phi_{xx}+2a^2\phi_{rr}=0 \tag{3}$$

The equation is to be solved subject to the boundary conditions that

$$\left.\begin{matrix}u\to 1\\ v\to 0\end{matrix}\right\} \text{ as } x^2+r^2\to\infty \tag{4a}$$

outside the nacelle, and that

$$u\to 1+k,\ v\to 0 \tag{4b}$$

inside the nacelle at the compressor face. The parameter k is related to the mass flow ratio $\bar{Q}=A_0/A_{hl}$ by the implicit formula

$$k=(A_{hl}/A_{cf})\bar{Q}[1-(\gamma-1)M_\infty^2(2k+k^2)/2]^{-1/\gamma-1}-1 \tag{5}$$

which is obtained using the isentropic relations.

The velocity potential is singular at infinity outside the nacelle. To remove this singularity, the contribution of the uniform stream is subtracted out, and a reduced potential G is defined such that

$$G=\phi-x \tag{6}$$

The boundary condition inside the nacelle, Eq. (4b), is applied at a finite distance representing the compressor face. The equation for the reduced potential is thus

$$(a^2-u^2)G_{xx}-2uvG_{xr}+(a^2-v^2)G_{rr}+a^2v/r=0 \tag{7}$$

where now $u=G_x+1$, $v=G_r$, and, on the axis,

$$(a^2-u^2)G_{xx}+2a^2G_{rr}=0 \tag{8}$$

On the axis of symmetry, we also must apply the boundary condition

$$G_r=0 \tag{9}$$

and, at points lying on the body surface, the inviscid boundary condition requires

$$v/u=\tan\theta_b \tag{10}$$

where θ_b is the local body inclination angle relative to the x axis.

Geometrical Considerations

The numerical calculation is performed on a rectangular domain, obtained from the original coordinates in the physical plane by a series of transformations. We denote the variable in the physical plane as $z=x+ir$, where x,r are the axial and lateral variables, respectively, in any azimuthal plane, and the coordinates are scaled such that point $(1,\pi)$ lies just inside the leading edge of the nacelle. The region outside the nacelle surface first is mapped to an infinite strip of slowly varying width by the conformal transformation

$$z=Z-\exp(-Z) \tag{11}$$

If we denote the real and imaginary parts of Z by X and Y, respectively, then the width of the strip in the Y direction is nearly equal to π, while the limit as $X\to-\infty$ corresponds to infinity in the physical plane outside the nacelle, and the limit as $X\to+\infty$ corresponds to infinity in the physical plane inside the nacelle.

In order to provide a simple, rectangular domain for the numerical calculation, the width of the strip is next made constant by the shearing transformation $\xi=X$, $\eta=Y/S(X)$, where $S(X)$ is the width of the strip as a function of X, which can be calculated from the nacelle coordinates and the transformation according to Eq. (11). Setting $T(X)=1/S(X)$, the equation for the reduced potential in this coordinate system becomes

$$\begin{aligned}&(a^2-U^2)G_{\xi\xi}+[2\eta_X a^2-2U\bar{V}]G_{\xi\eta}+[a^2(\eta_X{}^2+T^2)\\&-\bar{V}^2]G_{\eta\eta}+[\eta_{XX}(a^2-U^2)-2UVT']G_\eta\\&+P(U^2-V^2)+2UVQ-[(U^2+V^2)/h][(R^2+P)U\\&+QV]-[a^2h/(Y+Q)][QU-(1+P)V]=0\end{aligned} \tag{12}$$

where

$$U=[G_\xi+\eta(T'/T)G_\eta+1+P]/h \tag{13a}$$

$$V=[TG_\eta+Q]/h \tag{13b}$$

and

$$\bar{V}=TV+U\eta_X \tag{13c}$$

Here P and Q are the real and imaginary parts of $\exp(-Z)$, respectively, $R=\exp(-X)$, and

$$h^2=\left|\frac{dz}{dZ}\right|^2=1+2P+R^2$$

The body boundary condition, Eq. (10) in this coordinate system, becomes

$$G_\eta=-\frac{Q-S_X(G_\xi+1+P)}{T(1+S_X^2)} \tag{14}$$

to be applied along the line $\eta=1$.

Two final transformations are performed before the equation is cast in finite-difference form for solution. First, to remove the exponential behavior as $X\to-\infty$, we define $\zeta=X-\exp(-X)$. Then, to reduce the computational domain to a finite rectangle, we introduce the stretched coordinate $\bar{X}$ according to

$$\zeta=B(\bar{X}-C)/(1-\bar{X}^2)^A \tag{15}$$

whence $\bar{X}\to\pm1$ corresponds to $X\to\pm\infty$, i.e., infinity inside and outside the nacelle, respectively. A uniformly spaced, finite-difference grid is set up in the $(\bar{X},\eta)$ plane spanning the region $-1\le\bar{X}\le1$, $0\le\eta\le1$, which corresponds to the entire

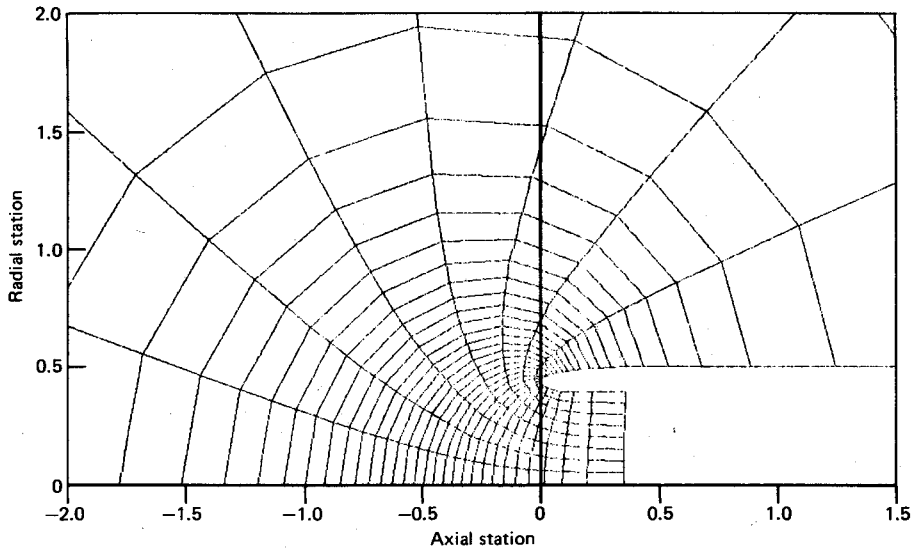

Fig. 2 Typical coordinate grid.

physical plane exterior to the nacelle surface. The constants A, B, and C are chosen to concentrate the mesh points in regions of high gradients. The distribution of mesh points in the vicinity of the nacelle lip is shown for a typical case in Fig. 2 for a grid containing 256 cells.

Finite-Difference Formulation

In the coordinate system developed in the preceding section, the flow is not always aligned, even approximately, with one of the coordinate directions. Therefore, a coordinate-invariant differencing scheme is required which always adds the artificial viscosity in a direction parallel to the velocity vector at supersonic points. Such a scheme has been developed by Jameson[5] and is the one we use. At supersonic points, the principal part of Eq. (12) is rewritten as

$$a^2 G_{nn} + (a^2 - q^2) G_{ss} = 0 \tag{16}$$

where n and s represent derivatives in the directions normal and parallel to the local velocity vector, and q is the magnitude of the velocity. In terms of the original coordinates,

$$G_{nn} = \frac{V^2}{q^2} G_{\xi\xi} + \frac{2}{q^2}(q^2 \eta_X - U\bar{V}) G_{\xi\eta} + \frac{1}{q^2}[q^2(\eta_X^2 + T^2) - \bar{V}^2] G_{\eta\eta} \tag{17a}$$

$$G_{ss} = \frac{U^2}{q^2} G_{\xi\xi} + \frac{2U\bar{V}}{q^2} G_{\xi\eta} + \frac{\bar{V}^2}{q^2} G_{\eta\eta} \tag{17b}$$

Upwind difference formulas then are used to represent the contributions to G_{ss}, while central difference formulas are used to evaluate contributions to G_{nn}.

The resulting difference equations can be solved by relaxation. In contrast to the simpler upwind difference schemes that can be used for the small-disturbance equations, however, the solution in the supersonic zone no longer can be obtained by marching, and special care is required in the construction of the iterative scheme to insure convergence. For this purpose, it is useful to regard the relaxation scheme as a discrete approximation to a time-dependent process, with the iterations as time steps. After dividing by a^2, the principal part of the equivalent time-dependent equation can be written as

$$G_{nn} + (1 - M^2) G_{ss} - 2\alpha G_{st} - 2\beta G_{nt} - 2\delta G_t = 0 \tag{18}$$

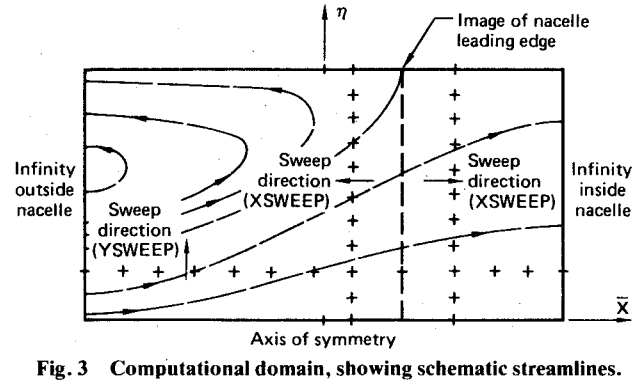

Fig. 3 Computational domain, showing schematic streamlines.

where M is the local Mach number q/a, and the values of α,β,δ depend upon the particular combinations of old and updated values of G used in the difference formulas. Then α should be positive so that the cone of dependence lies upstream of the n-t plane and behind the s-n plane. Also, to insure that s remains the timelike direction in the equivalent unsteady problem, α should satisfy the compatibility condition[5] $\alpha^2 > \beta^2 (M^2 - 1)$. Larger values of α lead to a more stable iteration but generally slower convergence. Finally, a local von Neumann test indicates that δ should be zero at supersonic points. At subsonic points, however, δ must be nonzero to provide the damping required for convergence of the successive overrelaxation scheme for elliptic operators.

Two alternative line-relaxation schemes incorporating these ideas were tested. In the first scheme, the equations are inverted simultaneously along lines of constant $\bar{X}$, sweeping the field to the right for lines intersecting the inner nacelle surface and to the left for lines intersecting the outer nacelle surface (see Fig. 3). This is necessary to avoid sweeping in the upstream direction at supersonic points, which are assumed to lie near the nacelle surface. In the second scheme, the equations are inverted simultaneously along lines of constant η, and the field is swept from the axis of symmetry to the nacelle surface. In general, it was found that the η-line scheme converged somewhat faster than the $\bar{X}$-line scheme in the pure relaxation mode, whereas the $\bar{X}$-line scheme seemed preferable in the hybrid method described in the next section.

Fast Iterative Schemes

The line overrelaxation schemes described in the previous section have the advantages of being quite stable and rapidly eliminating large errors in the initial estimates for the potential field, but their rates of convergence decrease as the

errors become smaller, with the result that convergence to very small residuals is excruciatingly slow, especially when the mesh spacing is small. This problem can be overcome partially by performing initial calculations on rather coarse grids and using these solutions as initial estimates for solutions on successively finer grids, as suggested by, e.g., South and Jameson[11] and Jameson.[12] Ultimately, however, more efficient methods are required to obtain highly converged solutions on fine grids. Two such methods are demonstrated on the present problem. The first is a hybrid method proposed by Jameson[13] in which a fast Poisson-solver is used in combination with relaxation; the second is an extrapolated relaxation scheme that takes advantage of the fact that the relaxation matrix has a dominant eigenvalue.

Hybrid Method

If Eq. (12) is divided by $a^2 T^2$, the linear portion is well represented by

$$(1/T^2)G_{\xi\xi} + G_{\eta\eta} \tag{19}$$

except near the axis, where it takes the form

$$(1/T^2)G_{\xi\xi} + 2G_{\eta\eta} \tag{20}$$

Let the correction to the potential at the kth iteration be defined as

$$C^{(k)} = G^{(k)} - G^{(k-1)}$$

and let $R(G^{(k)})$ denote the residual of the equation evaluated using values of G from the kth iteration. Then, if the linear terms dominate the equation, an iterative scheme in which $C^{(k+1)}$ is determined by solving the equation

$$(1/T^2)C^{(k+1)}_{\xi\xi} + C^{(k+1)}_{\eta\eta} = -\omega R(G^{(k)})/(a^2 T^2) \tag{21}$$

at each step can be expected to converge for some range of the parameter ω. The finite-difference form of Eq. (21) using central differences for the terms on the left-hand side can be solved directly using a fast Poisson-solver, since the grid spacing is constant in the η direction. Thus a very high computational efficiency can be realized. Unfortunately, the linear terms do not dominate the equation in the supersonic zone, and a local von Neumann test indicates that such an iterative procedure becomes unstable at supersonic points, even if upwind difference formulas are used in calculating the residuals R on the right-hand side of Eq. (21). Numerical experiments confirm this conclusion. The procedure can be stabilized by desymmetrizing the operator on the left-hand side of Eq. (21) for cases in which a nonrotated, type-dependent formulation can be used, e.g., when treating the transonic small-disturbance equations.[14] When the complexity of the problem requires a rotated scheme, however, this destroys the regularity of the iteration matrix required for use of the fast Poisson-solver, and much of the advantage of the method is lost.

Although this direct inversion scheme is unstable in supersonic regions, it is possible to use the inherent stability of the conventional relaxation process to overcome this, resulting in a scheme that is stable overall. Jameson has shown that, for the planar potential equation in a conformally mapped computational plane, if each Poisson step is followed by sufficient relaxation steps, the process again converges,[13] generally much faster than if the relaxation procedure is used alone.

Such a procedure is used here, using the Buneman algorithm[15] to invert Eq. (21), followed by p relaxation sweeps of the field. In general, $\omega = 0.75$ and $p = 5$ seem to give good rates of convergence for most problems thus far attempted.

Extrapolated Relaxation

It is well known that the convergence rate of relaxation schemes suffers as the mesh spacing goes to zero, because the spectral radius of the relaxation matrix then approaches unity for most elliptic problems. Suppose that the relaxation matrix has distinct eigenvalues, ordered such that $1 > |\lambda_1| > |\lambda_2| > \cdots > |\lambda_N|$. Then, after many iterations, the error vector, defined as $e^{(k)} = G - G^{(k)}$, where G is the exact solution, approaches the eigenvector corresponding to the dominant eigenvalue, so that

$$e^{(k+1)} \sim \lambda_1 e^{(k)} \tag{22}$$

Since the spectral radius $|\lambda_1|$ is nearly unity for the mesh spacings typically used, the final rate of convergence is slow. A procedure using the behavior just described to extrapolate relaxation solutions to very small residuals apparently was proposed first by Lyusternik[16] (see Forsythe and Wasow[17]) and also has been considered by Hafez and Cheng.[18] The idea is based upon the fact that

$$e^{(k+1)} - e^{(k)} = -C^{(k+1)}$$

whence the use of Eq. (22) gives

$$e^{(k)} = C^{(k+1)}/(1-\lambda_1)$$

In order to remove the error $e^{(k)}$ remaining after k iterations, this suggests that, in situations where Eq. (22) holds, one ought to add $C^{(k+1)}/(1-\lambda_1)$ instead of $C^{(k+1)}$ at the $(k+1)$st iteration. This corresponds to using a very large overrelaxation factor (of the order of hundreds or even thousands for typical problems).

In nonlinear problems of practical interest, it is difficult, if not impossible, to estimate λ_1 a priori (or even to predict whether there will, indeed, be a dominant eigenvalue of the relaxation matrix). However, assuming that such a dominant eigenvalue does exist, the fact that

$$C^{(k+1)}/C^{(k)} = e^{(k)}/e^{(k-1)} = \lambda_1 \tag{23}$$

provides a convenient method of determining its value as the iteration proceeds. During each relaxation sweep, the correction at each point is compared with that from the preceding sweep. If, at the end of the sweep of the entire field, the standard deviation (or some other statistical measure of the variance) of the values from the calculated mean $\bar{\lambda}$ is less than some fixed value, a dominant eigenvalue is judged to exist, and a new correction, equal to $\bar{\lambda}/(1-\bar{\lambda})$ times the most recent correction, is added to the potential at each point.

Results

Results of calculations performed using the analysis described in the preceding sections now will be presented. First, results of calculations will be compared with experimental data for several nacelle geometries, Mach numbers, and mass flow ratios. Second, results illustrating the advantages of the two types of iterative acceleration will be presented for a single (typical) test case. For all results presented, calculations were performed on a grid containing 128 mesh cells in the $\bar{X}$ direction and 32 mesh cells in the η direction. In some cases, preliminary calculations were performed on 32×8 and 64×16 grids, and the results of these solutions were used to provide starting data for the calculations on finer grids.

The calculations were performed on CDC 6500 and CDC 6600 machines. For the fine grid (128×32), a single relaxation sweep of the field requires typically 0.63 sec CPU time on the 6600 and about six times that amount on the slower 6500. The Poisson-solver step requires slightly more than twice the time of one relaxation sweep on the coarse grid and somewhat less than three times that of one relaxation sweep on the fine grid.

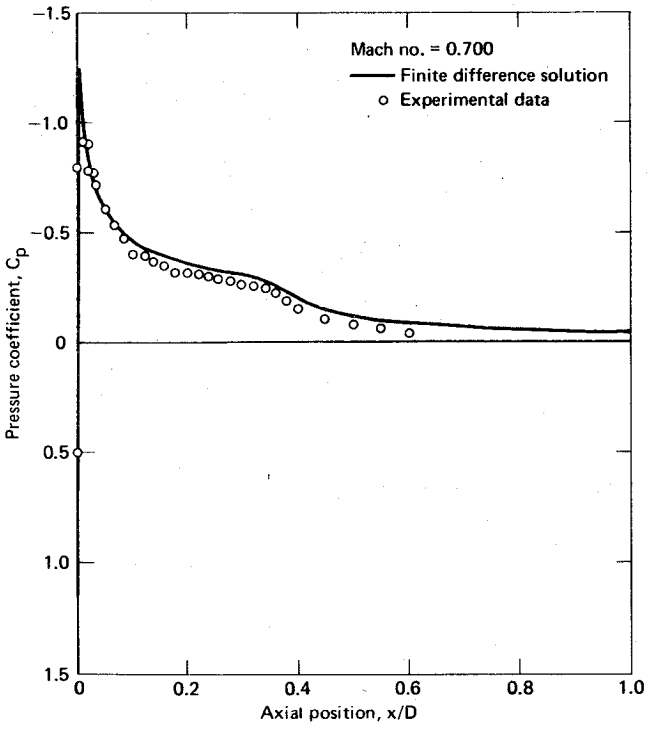

Fig. 4 Pressure distribution on cowl 36.

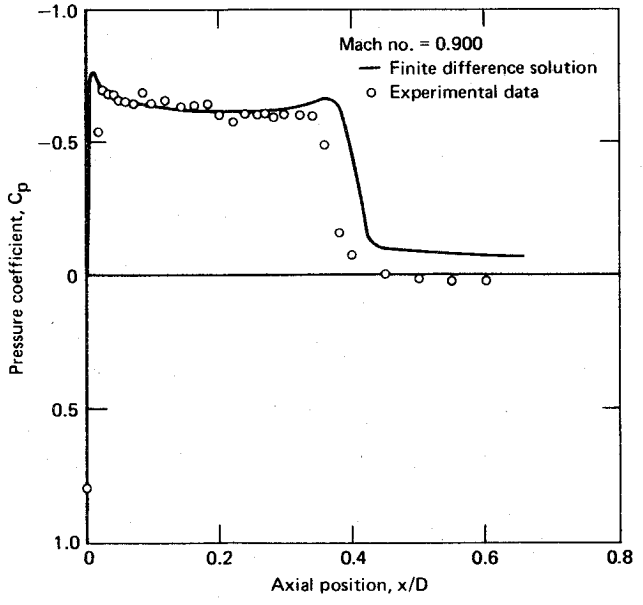

Fig. 5 Pressure distribution on cowl 36.

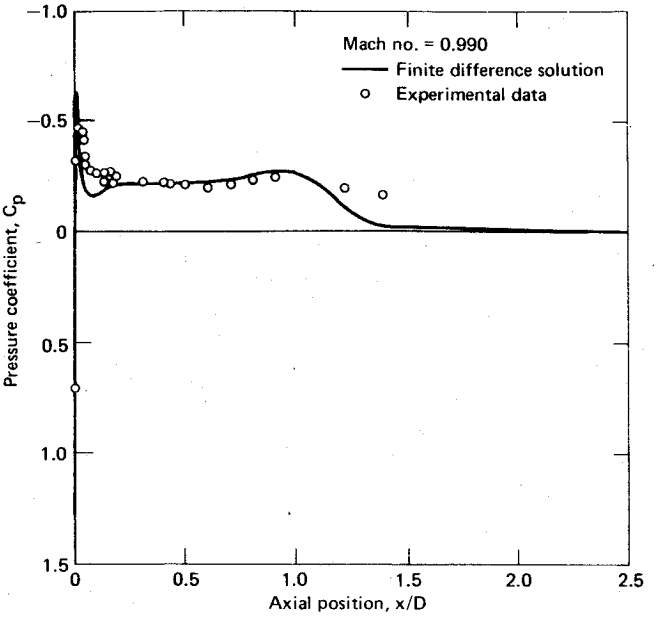

Fig. 6 Pressure distribution on cowl 1-85-100.

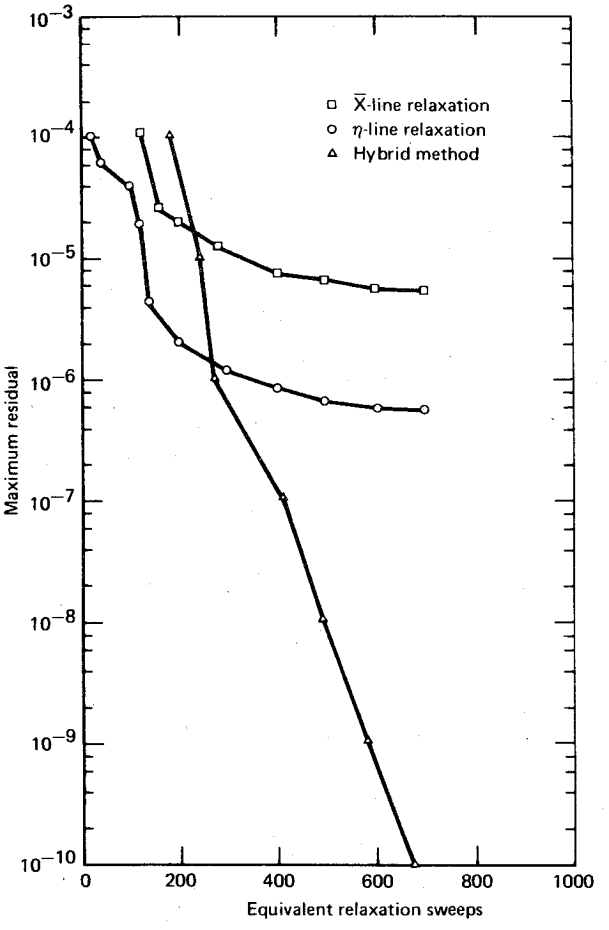

Fig. 7 Convergence rate of hybrid method.

Comparisons with Experimental Data

Figures 4 and 5 present comparisons of pressure distributions on the outside surface of a research cowl designed and tested by the Douglas Aircraft Company,[19] the shape of which is shown in Fig. 2. The two cases are for approximately the same mass flow ratio of $\bar{Q}=0.700$ and show the flow development with increasing Mach number. Agreement of the calculated results with the measured data is quite good, even in the absence of corrections for viscous effects.

Figure 6 presents results for an NACA 1-series cowl tested by Re.[20] The comparison presented is for the 1-85-100 cowl with a 1.046 internal contraction ratio operating at a mass flow ratio of 0.8073. The pressure distribution predicted by the present method is compared with that experimentally measured at a freestream Mach number of 0.99. The plateau pressure over most of the nacelle is well predicted, although the shock location is predicted too far forward. The location of the shock in the experiment was apparently farther downstream than the last pressure orifice on the model.

Accelerated Iterative Methods

Figure 7 illustrates the improved convergence rate of the hybrid method over those of the two conventional successive-

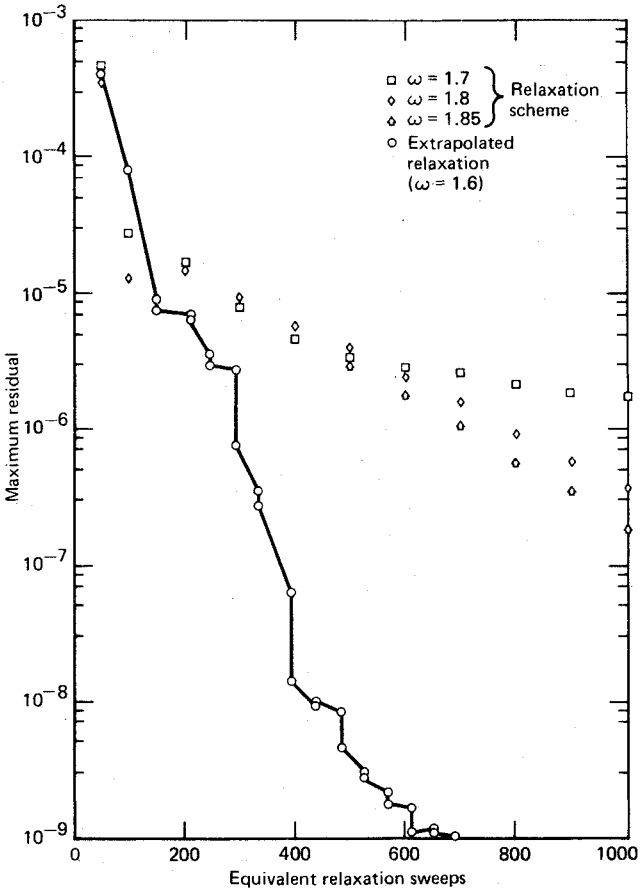

Fig. 8 Convergence of $\bar{X}$-line schemes.

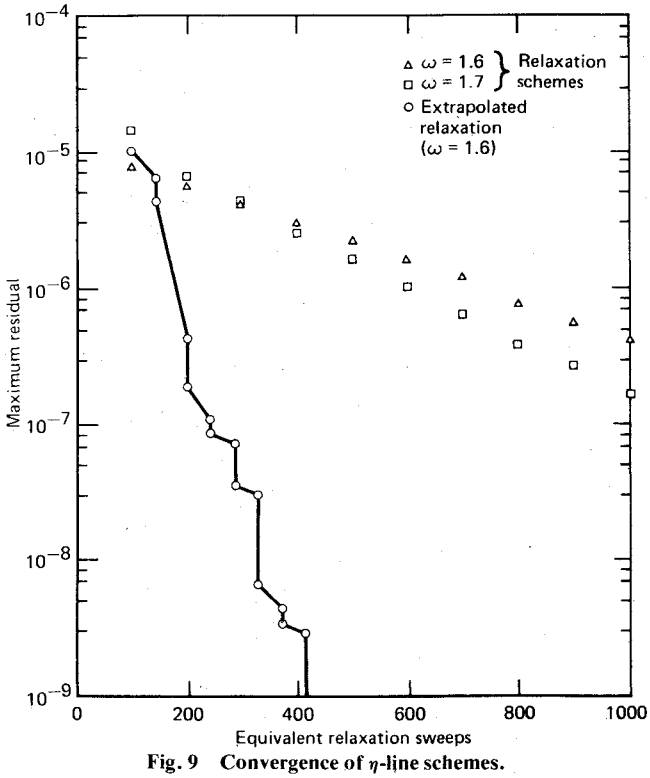

Fig. 9 Convergence of η-line schemes.

line-overrelaxation schemes for the case of Fig. 5. The largest absolute value of the residual is taken as a measure of convergence of the solution and is plotted as a function of computing time (expressed in terms of equivalent relaxation sweeps of the field). For residuals less than about 10^{-6}, the convergence rates of the relaxation schemes decrease rapidly, whereas that of the hybrid method remains approximately constant. This convergence rate may reasonably be expected to continue until roundoff error is encountered (at levels of about 10^{-14} on the CDC machines).

Figures 8 and 9 illustrate the improved convergence rates of the extrapolated relaxation schemes for the same case (but on the 64×16 grid). Figure 8 compares results for the $\bar{X}$-line scheme, and Fig. 9 compares results for the η-line scheme. In each case, the extrapolated version of the scheme converges to small residuals faster than the conventional version for all fixed values of the overrelaxation factor ω used. For each scheme, calculations were performed for a number of values of ω, gradually increasing them until instability occurred.

The accelerated methods are particularly useful if convergence to very small residuals is desired. In our calculations, the residuals are normalized by multiplying by $(\Delta\bar{X})^2$, so that they have the same order of magnitude as the corrections in a line relaxation sweep. With this normalization, the error resulting from incomplete convergence can be expected to be of the same order of magnitude as the discretization error when the residuals are reduced to $\sim(\Delta\bar{X})^{2+\alpha}$, where α is the order of accuracy of the difference scheme. Since α is 1 in the supersonic zone and 2 in the subsonic zone, the required level of the residual should be less than 10^{-6} on the fine grid. Such levels can be reached easily with the accelerated methods but only at great expense by relaxation.

Conclusion

The method presented converges rapidly to solutions of a finite-difference approximation to the complete potential equation for the inviscid, supercritical flow about inlet nacelles, and results agree well with experimentally measured pressure distributions for a variety of Mach numbers and mass flow ratios. Methods for accelerating the convergence of the iterative solution process are particularly useful when convergence to very small residuals is required.

The use of a nonconservative differencing scheme is justified on the basis of comparisons with experiment (see also Ref. 10), but a more rational treatment of the potential problem must use a conservation form of the equations and include a treatment of at least the displacement effect of the boundary layer. Such a conservation form easily might be incorporated into the present program along the lines of the analysis of Jameson.[9] The method also might be extended to treat symmetric planar inlets and problems in which the freestream is supersonic. These extensions would involve modifications of the singularity and the boundary condition at infinity outside the nacelle.

Acknowledgment

This work was supported in part by the Independent Research and Development Program of the McDonnell Douglas Corporation, and also by NASA under Grant NGR 33-016-167. Some of the calculations were performed at the ERDA Mathematics and Computing Laboratory, New York University, under Contract E(11-1)-3077.

References

[1] Murman, E.M. and Cole, J.D., "Calculation of Plane Steady Transonic Flows," *AIAA Journal,* Vol. 9, Jan. 1971, pp. 114-121.

[2] Garabedian, P.R. and Korn, D.G., "Analysis of Transonic Airfoils," *Communications in Pure and Applied Mathematics,* Vol. 24, 1972, p. 841.

[3] Jameson, A., "Transonic Flow Calculations for Airfoils and Bodies of Revolution," Grumman Aerodynamics Rept. 370-71-1, Dec. 1971.

[4] Ballhaus, W.F. and Bailey, F.R., "Numerical Calculation of Transonic Flow about Swept Wings," AIAA Paper 72-677, 1972.

[5] Jameson, A., "Iterative Solution of Transonic Flows over Airfoils and Wings, Including Flows at Mach 1," *Communications in Pure and Applied Mathematics,* Vol. 27, 1974, p. 283.

[6] Colehour, J.L., "Transonic Flow Analysis Using a Streamline Coordinate Transformation Procedure," AIAA Paper 73-657, 1973.
[7] Arlinger, B.G., "Calculation of Transonic Flow Around Axisymmetric Inlets," *AIAA Journal*, Vol. 13 Dec. 1975, pp. 1614-1621.
[8] Murman, E.M., "Analysis of Embedded Shock Waves Calculated by Relaxation Methods," *Proceedings, AIAA Computational Fluid Dynamics Conference,* pp. 27-40, July 1973; also *AIAA Journal*, Vol. 12, May 1974, pp. 626-633.
[9] Jameson, A., "Transonic Potential Flow Calculations Using Conservation Form," *Proceedings, AIAA 2nd Computational Fluid Dynamics Conference,* pp. 148-155, June 1975.
[10] Bauer, F. and Korn, D., "Computer Simulation of Transonic Flows Past Airfoils with Boundary Layer Correction," *Proceedings, AIAA 2nd Computational Fluid Dynamics Conference*, pp. 184-189, June 1975.
[11] South, J.C., Jr. and Jameson, A., "Relaxation Solutions for Inviscid Axisymmetric Transonic Flow over Blunt or Pointed Bodies," *Proceedings, AIAA Computational Fluid Dynamics Conference,* pp. 8-17, July 1973.
[12] Jameson, A., "Numerical Calculation of the Three-Dimensional Transonic Flow over a Yawed Wing," *Proceedings, AIAA Computational Fluid Dynamics Conference*, pp. 18-26, July 1973.
[13] Jameson, A., "Accelerated Iterative Schemes for Transonic Flow Calculations using Fast Poisson-Solvers," New York Univ. ERDA Rept. C00 3077-82, April 1975.
[14] Martin, E.D., "A Fast Semidirect Method for Computing Transonic Aerodynamic Flows," *Proceedings, AIAA 2nd Computational Fluid Dynamics Conference*, pp. 162-174, June 1975.
[15] Buzbee, B.L., Golub, G.H., and Nielsen, C.W., "On Direct Methods of Solving Poisson's Equation," *SIAM Journal of Numerical Analysis*, Vol. 1, 1970, p. 627.
[16] Lyusternik, L.A., "Zamechania k chislemomu resheniyu kraevykh zadach uravnenia Laplasa i vychisleniyu sobstvennykh znachenii metodom setok," *Matematicheskii Institut imeni V.A. Steklova, Trudy*, Vol. 20, 1947, p. 49.
[17] Forsythe, G.E. and Wasow, W.R., *Finite-Difference Methods for Partial Differential Equations*, Wiley, New York, 1960.
[18] Hafez, M.M. and Cheng, H.K., "Convergence Acceleration and Shock Fitting for Transonic Flow Computations," Univ. of Southern California Rept. USCAE-132; supercedes AIAA Paper 75-51, 1975.
[19] Ambrosiani, J., unpublished data, Douglas Aircraft Co., Long Beach, Calif.
[20] Re, R.J., "An Investigation of Several NACA 1-Series Axisymmetric Inlets at Mach Numbers from 0.4 to 1.29," NASA TM X-2917, March 1974.